Available online at www.sciencedirect.com

ScienceDirect

Energy Procedia 81 (2015) 704 – 714

Energy Procedia

69th Conference of the Italian Thermal Engineering Association, ATI 2014

Employment of an Auto-Regressive Model for Knock Detection supported by 1D and 3D Analyses

Siano D.[a], Severi E. [b], De Bellis V.[c]*, Fontanesi S. [b], Bozza F. [c]

[a] *Istituto Motori CNR, Naples, Italy*
[b] *Department of Engineering "Enzo Ferrari", University of Modena and Reggio Emilia, Italy*
[c] *Industrial Engineering Department, University of Naples "Federico II", Naples, Italy*

Abstract

In this work, experimental data, carried out on a twin-cylinder turbocharged engine at full load operations and referred to a spark advance of borderline knock, are used to characterize the effects of cyclic dispersion on knock phenomena. 200 consecutive in-cylinder pressure signals are processed through a refined Auto-Regressive Moving Average (ARMA) mathematical technique, adopted to define the percentage of knocking cycles, through a prefixed threshold level. The heuristic method used for the threshold selection is then verified by 1D and 3D analyses.

In particular, a 1D model, properly accounting for cycle-by-cycle variations, and coupled to a reduced kinetic sub-model, is used to reproduce the measured cycles, in terms of statistical distribution of a theoretical knock index. In addition, few individual cycles, representative of the whole dataset, are selected in a single operating condition in order to perform a more detailed knock analysis by means of a 3D CFD approach, coupled to a tabulated chemistry technique for auto-ignition modeling.

Outcomes of 1D and 3D models are compared to the ARMA results and a substantial coherence of the numerical and experimental results is demonstrated. The integrated 1D and 3D analyses can hence help in supporting the choice of the experimental threshold level for knock identification, following a more standardized theoretical approach.

Peer-review under responsibility of the Scientific Committee of ATI 2014

Keywords: knock detection; internal combsution engine; Auto-Regressive Moving Average model; 1D modeling; 3D modeling

* Corresponding author. Tel.: +39-081-7683264; fax: +39-081-2394165.
E-mail address: vincenzo.debellis@unina.it

Peer-review under responsibility of the Scientific Committee of ATI 2014
doi:10.1016/j.egypro.2015.12.076

Nomenclature

1D, 3D	One, three-dimensional
AIC	Akaike information criterion
AIHRR	Auto-ignition heat release rate
ARMA	Auto-regressive moving average
CV	Cyclic variation
ICE	Internal combustion engine
IMEP	Indicated mean effective pressure
LES	Large eddy simulation
LHV	Lower heating value
MAPO	Maximum amplitude pressure oscillation
NV	Noise variance
PMHRR	Pre-mixed heat release rate
RANS	Reynolds averaged Navier-Stokes
RON	Research octane number
SI	Spark ignition
e_i	Prediction error
m	MA order
m_f	Fuel mass
n	AR order
N	Number of samples
Q_{chem}	Auto-ignition heat
t	Time
x_i	Time signal
x_{Qchem}	Normalized auto-ignition heat
Y_{IG}	Precursor concentration
Y_{TF}	Fuel tracer concentration
θ	Engine crank angle
μ	Mean value
σ^2	Noise variance

1. Introduction

Knock is one of the most critical factors that limit the spark ignition (SI) performance of a downsized internal combustion engine (ICE) at full load operations. As known, knock arises when a portion of the fuel charge within the combustion chamber spontaneously ignites after the spark event, but before it has been reached by the flame front propagating from the spark plug, [1], [2]. This phenomenon most likely occurs within the air/fuel charge molecules that burn late during the combustion process (end-gas auto-ignition). This issue becomes more critical in SI turbocharged engines, where the in-cylinder temperature and pressure are higher.

Knock phenomena, moreover, are largely affected by cycle-to-cycle variation (CV). As known, CV is mainly a consequence of the early flame development conditions, that deeply influence the subsequent combustion phase [3], [4]. The flame kernel formation in fact depends on thermo-fluid-dynamic conditions at the spark plug location, affected by the spatial and temporal fluctuations of the turbulent flow field inside the cylinder. For the above reasons, individual cycles, characterized by increased burning rates, are most likely to exhibit knock.

Because of CV, the knock extent must be hence quantified following a statistical approach. The experimental identification of the “knocking” combustions requires the measurement of numerous instantaneous pressure cycles, at a high crank angle resolution (usually 0.1 degrees). A careful treatment of the measured data must be then performed to estimate a proper knock index from the analysis of each instantaneous pressure cycle [5], [6]. Usually, a certain operating condition is assumed as “knocking” when a prefixed percentage of individual cycles (around 2-

3%) is characterized by a knock index overtaking a predefined threshold level. The latter comes out from a number of considerations based on extensive engine calibration at the test-bench, manufacturer know-how, durability tests, etc. The whole process is affected by a certain arbitrariness, according to the employed data processing technique, proper definition of the threshold level, accepted percentage of knocking cycles, etc. In particular, especially in the case of absence of extensive durability tests, the choice of the threshold level is a very critical issue since it usually depends on the engine speed and load conditions.

For the above considerations, it is important to try to support the experimental activity with advanced 1D and 3D numerical analyses. However, CV cannot be easily predicted by a numerical model. In a 1D approach, CV can be indeed "imposed" through a perturbation of the parameters that control the combustion phase and duration [7]-[10]. Knock occurrence can be then detected by either Arrhenius-like induction time correlations [11], [12], or solving a reduced kinetic scheme in the unburned gas zone [13]. On the contrary, more complex 3D LES simulations showed the potential to properly describe CV phenomenon [14], [15]. This last approach is however very time-consuming, especially if coupled to detailed chemical kinetics [16].

In this work, a preliminary experimental campaign is carried out in order to characterize the engine behavior of a commercial small-size twin-cylinder turbocharged SI engine at full load operation under incipient knocking conditions. Main features of the analyzed engine are reported in Table 1.

For each tested speed, a sequence of 200 consecutive cycles are acquired and processed by an Auto-Regressive Moving Average (ARMA) technique. Then, a 1D numerical methodology is proposed with the aim to statistically reproduce the train of measured pressure traces, and to analyze the combustion process and the knock occurrence in presence of cyclic variability. Finally, in order to save computing time, only few cycles, representative of the whole 200 dataset, are analyzed by means of a 3D simulation employing a tabulated chemistry technique. The experimental and numerical knock indices are finally compared, denoting a substantial coherence and agreement.

Table 1. Main features of the downsized engine under test

Engine Model	2 Cylinders, 8 valves, VVA
Stroke/Bore/Displacement	86 mm / 80.5 mm / 875 cm^3
Connecting rod length	136.85 mm
Compression Ratio	9.9
Max Brake Power	64.6 kW @ 5500 rpm
Max Brake Torque	146.1 Nm @ 2500 rpm

2. ARMA model description

As known, a commonly used knock detection is based on the high frequency filtering of in-cylinder measurements (MAPO index [17]-[19]). In the present paper, indeed, an alternative ARMA approach is applied, which was proven to better perform particularly under soft-knock conditions [20]. Objective of an ARMA model is to predict the actual value of time signal x_t, based on its past history (AR property) and adding a prediction error (e_t) in the form of a Moving Average (MA) The following equation hence defines an ARMA model with an AR order of n and a MA order of m:

$$x_t + a_1 x_{t-1} + ... + a_n x_{t-n} = e_t + b_1 e_{t-1} + ... + b_m e_{t-m} \quad (1)$$

An ARMA(n,m) model is hence constituted by $n+m$ coefficients, which must be selected to minimize the prediction error, e_t. Different techniques can be followed to estimate the above coefficients. Among these, Yule-Walker functions or a least-squares polynomial regression are the most employed ones [21]. The accuracy level of the ARMA model is then synthesized in terms of variance of the error function, or Noise Variance (NV), defined as the sum of the squared distances of each term in the error function series from the mean (μ), divided by the number of samples, N:

$$\sigma^2 = \frac{\sum (e_t - \mu)^2}{N} \tag{2}$$

The smaller NV, the better the estimated model fits the time series. On the contrary, changes in the variance of the prediction error identify the presence of physical phenomena altering the characteristics of the time series. This property is here utilized to identify knocking phenomena. In particular, the in-cylinder data represent the time series (x_t), directly affected by uncorrelated disturbances (knocking, e_t). Knock phenomena will cause substantial deviations of the error function from its mean value. By monitoring the NV level, it is hence definitely possible to detect the knock occurrence and its intensity, even in the case of incipient knocking conditions.

It must be stressed however that a suitable ARMA model should be made up of the smallest number of adjustable parameters ($n+m$) that can achieve the desired accuracy. For this reason, it is very important to also define a criterion for the selection of the optimal model orders, n and m [22], [23]. In the present analysis, the Akaike Information Criterion (AIC) is used [24], given by:

$$AIC = \log\left[\sigma^2\right] + \frac{2(n+m)}{N} \tag{3}$$

In the above definition, the first term is a decreasing function of the model orders, while the second has an opposite trend, and represents a penalty adjustment. Since a proper ARMA(n,m) model should realize the lowest variance with the minimum number of parameters, the AR and MA orders reaching the lowest AIC level must be searched. In particular, the order selection is performed as follows:

1. The ranges of the ARMA model orders to be considered are selected (e.g. $1 \leq n \leq n_{max}$ and $1 \leq m \leq m_{max}$); in this case $n_{max}=m_{max}=8$.
2. For each order pair (n,m), the coefficients of the ARMA model are estimated.
3. Based on the selected AIC criterion, the prediction error variance is calculated for each pair.
4. Finally, the (n,m) order pair that yields the lowest value of the selected criterion is chosen as the optimal pair.

A Matlab™ routine was in house developed in order to identify the best model order. The method has been applied to a complete time series, involving more than 200 cycles in a single operating condition (1500 rpm, cylinder 2). To exclude knock unrelated phenomena, each individual cycle is only processed in the crank angle window (10, 75 CAD).

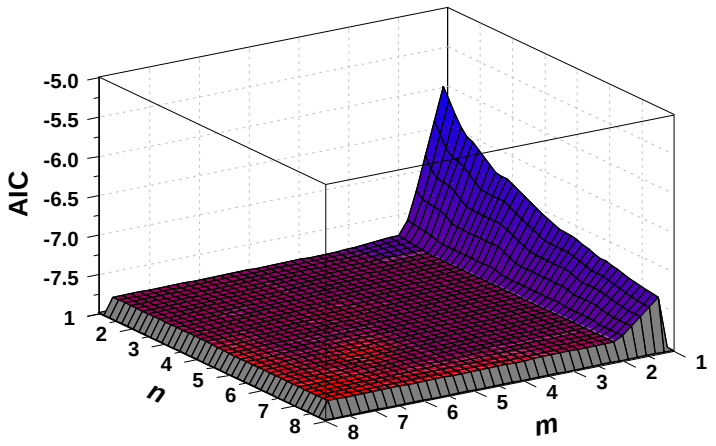

Fig. 1. AIC Surface plot

Fig. 1 shows the obtained AIC surface plot. Initially, by increasing both *n* and *m*, the AIC index rapidly reduces, while further increases in both orders only realize negligible improvements. The minimum AIC value is obtained with *n*=3 and *m*=2, which hence represent the proper orders to be selected.

Once set up, the ARMA(3,2) model is applied to all the investigated operating conditions. A complete picture of the model outcomes is given in Fig. 2: it displays, at each engine speed, the cycle-by-cycle noise variance levels resulting from the processing of each individual cycle, [18]. A predefined null offset threshold level is also reported. Due to the presence of background pressure fluctuations at high speeds, a linearly increasing threshold would seem to be appropriate [25]. Its slope, as already discussed, cannot be not fully rigorous and mainly comes out from the analysis of some individual cycles exhibiting noise variance peaks [26], [27].

It can be noted that cylinder #1 presents knock free operations for almost all the considered speeds, while cylinder 2 shows a certain number of cycles above or very close to the threshold for all the considered speeds. The more critical speed is 2100 rpm, where the maximum percentage of knocking cycle occurs.

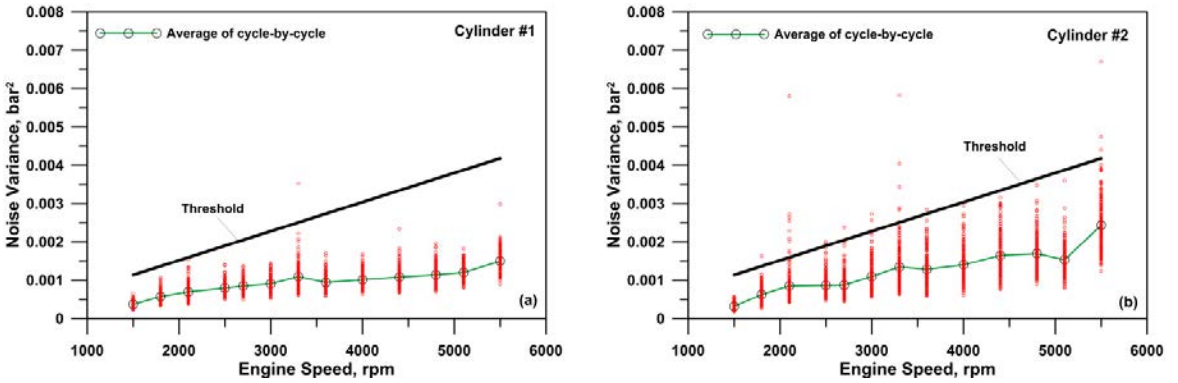

Fig. 2. Cycle-by-cycle noise variance for all investigated engine speeds, (a) cylinder #1, (b) cylinder #2

It is well known that the knocking combustions most likely occur when high in-cylinder pressure and temperature peaks are attained. Based on the this consideration, it appears possible to find a correlation between the assigned NV threshold and a peak pressure value above which knocking combustions begin to arise. With reference to the more critical speed of 2100 rpm, it can be observed in Fig. 3 that the cycles characterized by a NV above the threshold also present a peak pressure exceeding 68 bar. In the following sections, 1D and 3D simulations are used to support the NV threshold choice, numerically verifying the presence of knocking combustions for the cycles exhibiting a peak pressure above 68 bar.

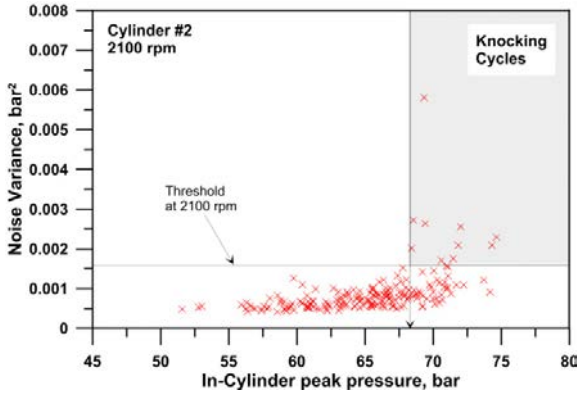

Fig. 3. ARMA analysis of the experimental pressure cycles at 2100 rpm

3. 1D model description and results

The model of the analyzed ICE is implemented in the well-known GT-Power software. In particular, a quasi-dimensional turbulent combustion model, based on a deeply validated fractal schematization of the flame surface [28]-[30] is employed. The combustion model is tuned with reference to “ensemble averaged” experimental pressure cycles and is then extended to include the CV effects. CV is taken into account by introducing proper random variations of the parameters listed in Table 2 [20]. The parameters variation range is specified in order to realize an IMEP standard deviation similar to the one observed in the experimental data. The experimental/numerical comparisons between the averaged IMEP and the related standard deviation are shown in Fig. 4, denoting a good agreement. It is not worthless to emphasize that the combustion and CV models tuning constants are kept unchanged for all the considered operating conditions.

Table 2. Range of variation of the cycle-by-cycle model parameters

Perturbed parameter	Range of variation
Δ Spark advance, deg	± 2.5
Δ Intake valve closure, deg	± 1.0
Δ Air-to-fuel ratio, -	± 0.1
Variation of turbulence intensity, %	± 17
Variation of flame kernel radius, %	± 50

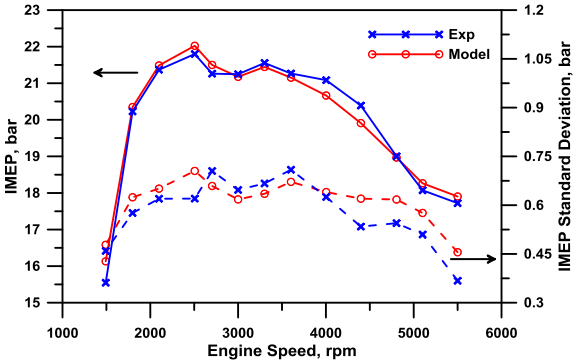

Fig. 4. Comparison between the experimental and simulated averaged IMEP and IMEP standard deviation [20]

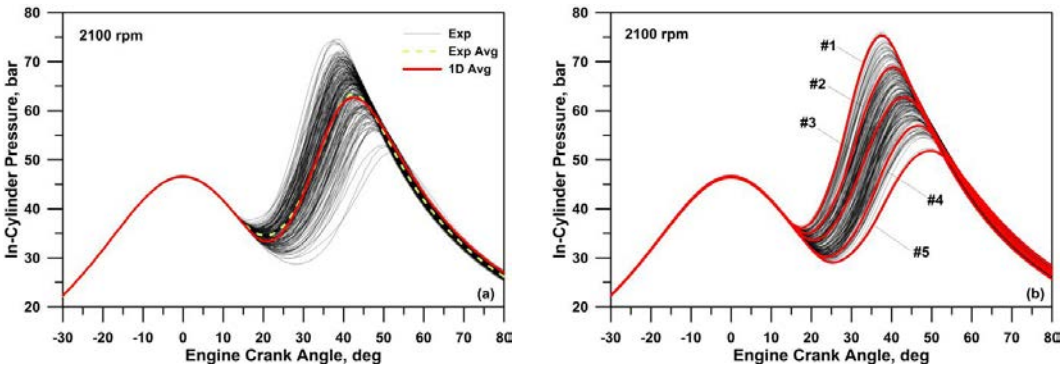

Fig. 5. Sequence of experimental pressure traces, its ensemble average and 1D mean pressure cycle (a), 1D simulated pressure cycles including cycle-by-cycle variation (b)

In Fig. 5a, the comparison between the measured and simulated ensemble-averaged pressure cycles at 2100 rpm are shown. This last speed, as stated above, is identified by the ARMA analysis as the most critical operating condition in terms of percentage of knocking cycles. The related train of 200 consecutive experimental cycles is also plotted Fig. 5a, to be compared to the simulated data set in Fig. 5b. Five modelled cycles are selected, characterized by a different peak pressure. In particular, cycles #1, #3 and #5 correspond to the maximum, mean and minimum peaks, respectively, while cycles #2 and #4 represent intermediate conditions. The above cycles will be used as a reference in the following 3D analyses, as well.

In order to estimate the knock intensity, the combustion and cyclic dispersion models are coupled to a chemical kinetic solver (CHEMKIN). In particular, the knock intensity is computed at each individual engine cycle, through the solution of a kinetic scheme inside the "end-gas" unburned zone [31]. The adopted knock index, labelled as x_{Qchem}, is defined as the ratio between the heat released in the unburned zone (Q_{chem}) and the overall heat available in the injected fuel (fuel mass, m_f, multiplied by the fuel lower heating value, LHV) (see eq. (4)). The adopted approach is widely described in [20].

$$x_{Qchem} = \frac{Q_{chem}}{m_f LHV} 100 \tag{4}$$

In Fig. 6, the NV indices derived by the ARMA analysis of the measured traces are compared with the x_{Qchem} index derived by the 1D simulated pressure cycles. The figure also reports the fittings (quadratic polynomial) of the above data. It can be observed that both the indices can be properly fitted by a curve increasing with peak pressure. In addition, the latter show a very similar trend.

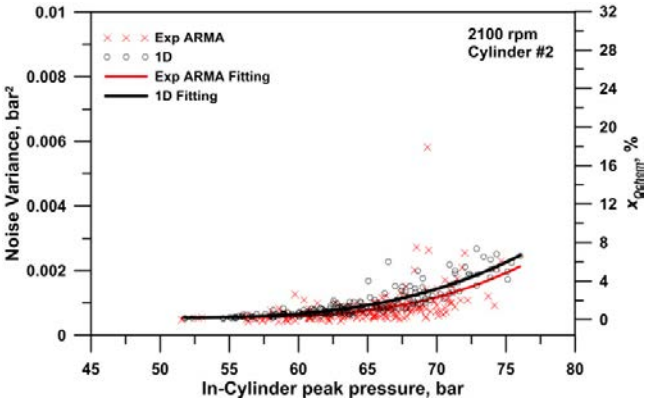

Fig. 6. Noise Variance and x_{Qchem} indices vs. in-cylinder peak pressure at 2100 rpm

The above results highlight the substantial coherence between the ARMA analysis processing the experimental data and the 1D approach. In the next section, 3D analyses will be proposed with the aim to further verify the NV threshold choice.

4. 3D model description and results

The computational domain of the 3D in-cylinder combustion analyses, which covers the combustion chamber and the port portions within the engine head, is built in Star-CD, licensed by CD-Adapco. Information about the 3D CFD model setup can be found in [29], [32] and are not recalled here for the sake of brevity.

The methodology adopted for the auto-ignition onset is based on a tabulated approach for the actual chemistry of real engine fuels proposed by the authors in [16]. Combustion is modelled using the built in ECFM-3Z model, auto-ignition is computed in the paper for a RON95 gasoline. The auto-ignition chemistry is tracked at a cell-wise level: for each computational cell and each time step, auto-ignition delays are extracted from the table by using a multi-

linear interpolating routine, and then used to evaluate the progress of auto-ignition pre-reactions, tracked through a transported passive scalar based on the correlation by Lafossas [33]:

$$\frac{dY_{IG}}{dt} = Y_{TF}\sqrt{1+\frac{4(1-\tau)}{\tau^2}\frac{Y_{IG}}{Y_{TF}}} \tag{5}$$

Auto-ignition occurs as soon as the precursor concentration Y_{IG} locally equates the fuel tracer concentration Y_{TF}. The validation of the combustion and knock CFD setup has been carried out through the comparison against experimental in-cylinder pressure traces, as widely reported in [32]. To the aim of roughly taking into account CV, while saving the RANS modelling framework, five individual cycles, representative of the 200 pressure signals experimentally acquired, are reproduced by the 3D model simply delaying or advancing the spark timing. Fig. 7 reports the comparison between the 3D in-cylinder mean pressure and the correspondent 1D traces denoting a satisfactory agreement. This is of course an important prerequisite to guarantee the comparability between the 1D and the following 3D knock analyses.

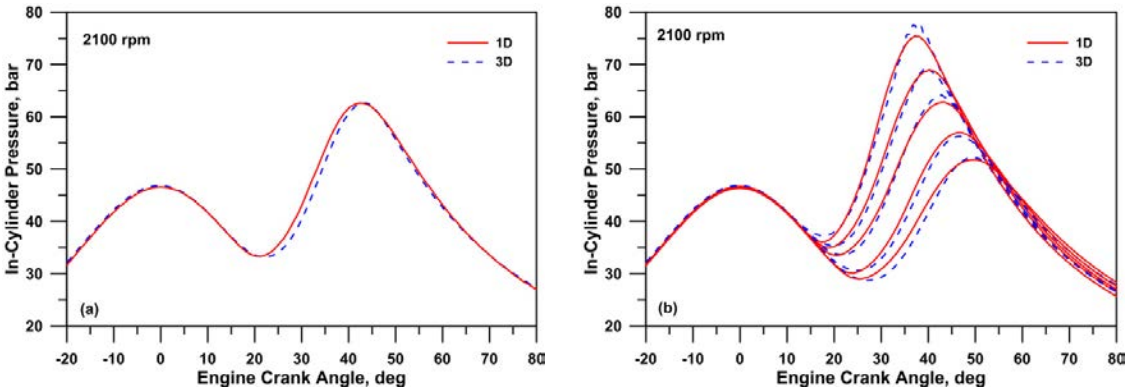

Fig. 7. Comparison between 3D and 1D in-cylinder pressure, average (a) and selected cycles representative of the cyclic variation.

Numerical data are also post-processed in terms of knock-related heat release and local in-cylinder pressure fluctuations. In particular, 8+1 pressure sensors are located on the periphery of the combustion chamber, as reported in Fig. 8. The one labelled as “Transducer” is representative of the actual pressure probe adopted during the tests at the test bench.

In Fig. 8, in-cylinder pressure fluctuations are reported for cycles #1-#4. In particular, cycle #1 shows the highest pressure oscillations and its peak pressure is well above the threshold level of 68 bar identified through the ARMA analysis. Smaller local pressure fluctuations characterize the cycle #2, that has a peak pressure almost equal to the threshold. Finally, negligible pressure fluctuations are detected for the cycles #3 and #4, having a peak pressure below the threshold.

The above results also point out that, among the various sensors, the maximum oscillations are detected by the sensor 4 for all the selected cycles. This highlights that the estimated knock-prone region is the portion of the combustion chamber pertaining to the exhaust valve named as “2”. As experimentally proved in [5], [34], it is numerically confirmed that a substantially different knock signature is obtained at different positions in the combustion chamber.

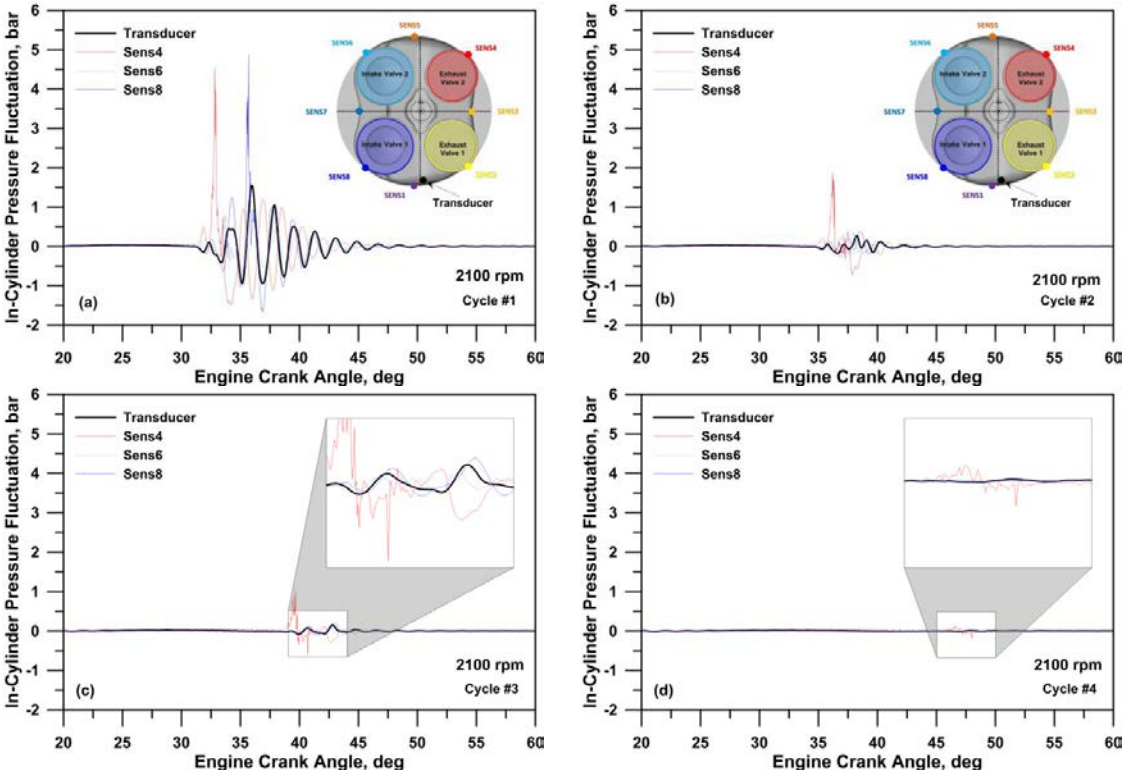

Fig. 8. Sensor locations and knock-related pressure fluctuations for cycle #1 (a), #2 (b), #3 (c) and #4 (d)

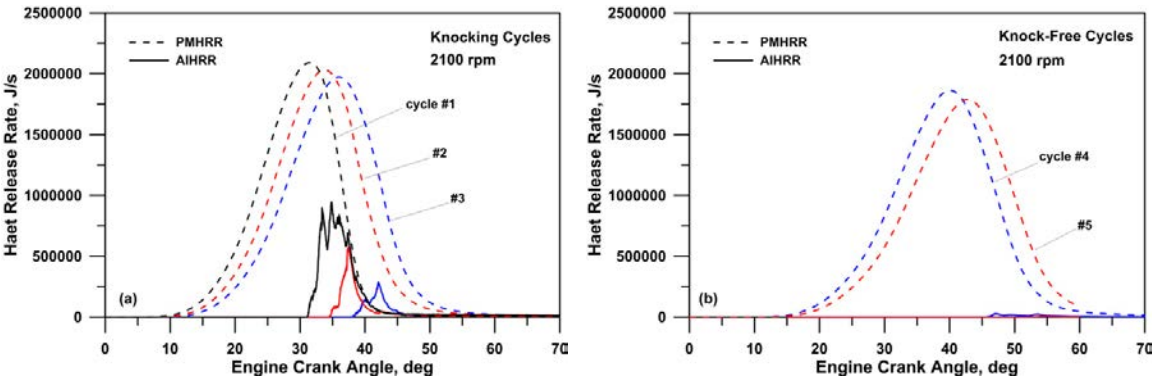

Fig. 9. Heat release due to premixed combustion and auto-ignition, cycles #1-5

A more objective knock indicator than the pressure fluctuations is represented by the heat released in the end-gas. The latter is depicted in Fig. 9 in terms of knock-related Auto-Ignition Heat Release Rate (AIHRR) and is compared with the “normal” combustion (premixed) HRR (PMHRR). Congruently with the previous discussion pertaining to the in-cylinder pressure oscillations, AIHRR becomes relevant for the cycles which exhibit a peak pressure above the threshold. In particular, for cycle #1, the AIHRR peak represents a significant percentage of the PMHRR one.

Similarly to 1D approach, it is possible to derive from the 3D results a knock index that quantify the auto-ignition heat normalized with the overall heat released, according to eq. (6).

$$x_{Qchem} = \frac{\int AIHRR\, d\theta}{\int AIHRR\, d\theta + \int PMHRR\, d\theta} 100 \tag{6}$$

In Fig. 10, the x_{Qchem} parameter derived by 1D and 3D simulations, eqs. (4) and (6), are compared. It can be noted that a similar trend is obtained, even if the 3D results present higher values for the same peak pressure. Of course, effects related to local heat transfer, chemical kinetics and temperature distribution inside the combustion chamber are the main responsible for the highlighted slight differences.

Results reported in Figures 6 and 11 demonstrate the substantial agreement between 1D, 3D and experimentally-derived data, and allow to support the initially heuristic choice of the noise variance threshold.

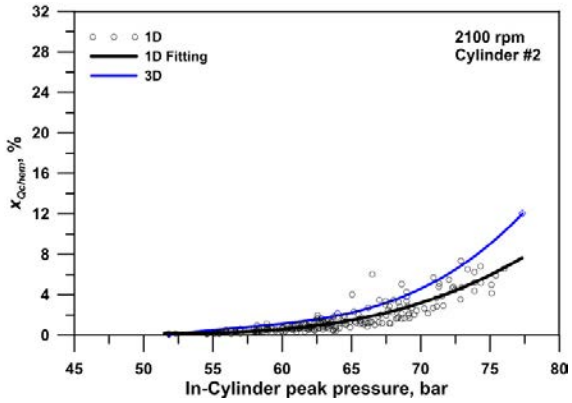

Fig. 10. x_{Qchem} computed by 1D and 3D simulations at 2100 rpm

5. Conclusions

The knock behavior of a small size spark ignition turbocharged VVA engine is analyzed by means of the ARMA technique, processing experimental in-cylinder pressure signals. After a preliminary set-up, a knock-related index, namely the noise variance, is computed for a sequence of 200 consecutive pressure cycles at each speed. Based on a heuristic definition of a threshold level, knock-prone cycles are detected. To support the choice of the threshold level, 1D and 3D analyses of the combustion and knock phenomena are carried out.

First, a 1D model is used to reproduce the engine performance, including cycle-by-cycle variations. To this aim, the model parameters are randomly perturbed to mimic the experimental IMEP standard deviation. The knock intensity is then computed for each simulated cycle coupling the combustion model to a chemical kinetic solver.

Five cycles, characterized by different pressure peaks, are then analyzed by a detailed 3D simulation. The latter puts into evidence that the pressure fluctuations related to the knocking combustion assume a different amplitude according to the location of the pressure sensor, resulting in an apparent different knock intensity. Finally, the knock indices derived by the 1D and 3D methodologies are compared with ARMA outcomes, denoting a substantial coherence with the choice of the noise variance threshold.

References

[1] Heywood, J.B., Internal Combustion Engine Fundamentals, McGraw-Hill Inc., New York, 1988.
[2] Hudson, C. et al., Knock measurement for fuel evaluation in spark ignition engines, *Fuel Journal* 80 (2001) 395–407.
[3] Stone, C. et al., Cycle-by-Cycle Variations in Spark Ignition Engine Combustion - Part II: Modelling of Flame Kernel Displacements as a Cause of Cycle-by-Cycle Variations, SAE Paper 960613, 1996, doi:10.4271/960613

[4] Holmström K., Denbratt I., Cyclic Variation in an SI Engine Due to the Random Motion of the Flame Kernel, SAE Paper 961152, 1996, doi:10.4271/961152
[5] Millo F., Ferraro C., Knock in S.I. Engines: A Comparison between Different Techniques for Detection and Control," SAE Paper 982477, 1998, doi:10.4271/982477.
[6] Cavina N. et al., Combustion Monitoring Based on Engine Acoustic Emission Signal Processing, SAE Paper 2009-01-1024, 2009.
[7] Pera, C. et al., Exploitation of Multi-Cycle Engine LES to Introduce Physical Perturbations in 1D Engine Models for Reproducing CCV, SAE Paper 2012-01-0127, 2012.
[8] Millo F. et al., A Methodology to Mimic Cycle to Cycle Variations and to Predict Knock Occurrence through Numerical Simulation, SAE Paper 2014-01-1070, 2014, doi:10.4271/2014-01-1070
[9] Sjeric M. et al., Experimentally Supported Modeling of Cycle-to-Cycle Variations of SI Engine Using Cycle-Simulation Model, SAE Paper 2014-01-1069, 2014, doi:10.4271/2014-01-1069
[10] Fontana G. et al., Experimental and Numerical Analyses for the Characterization of the Cyclic Dispersion and Knock Occurrence in a Small-Size SI Engine, SAE Paper 2010-32-0069 / 20109069, SETC 2010 Conference, Linz, September 2010.
[11] Livengood J. C., Wu, P. C., Correlation of Autoignition Phenomenon in Internal Combustion Engines and Rapid Compression Machines, Fifth Symposium (International) on Combustion, pp. 347-356, 1955
[12] Douaud A., Eyzat P., Four-Octane-Number Method for Predicting the Anti-Knock Behavior of Fuels and Engines, SAE Paper 780080, 1978, doi:10.4271/780080
[13] Siano D., Bozza F., Knock Detection in a Turbocharged S.I. Engine Based on ARMA Technique and Chemical Kinetics, SAE Paper 2013-01-2510, 2013, doi:10.4271/2013-01-2510
[14] Fontanesi S. et al., LES Analysis of Cyclic Variability in a GDI Engine, SAE Paper 2014-01-1148, 2014, doi:10.4271/2014-01-1148
[15] Fontanesi S. et al., Assessment of the Potential of Proper Orthogonal Decomposition for the Analysis of Combustion CCV and Knock Tendency in a High Performance Engine, SAE Paper 2013-24-0031, 2013, doi:10.4271/2013-24-0031.
[16] Fontanesi S. et al., Knock Tendency Prediction in a High Performance Engine Using LES and Tabulated Chemistry, *SAE Int. J. Fuels Lubr.* 6(1):98-118, 2013, doi:10.4271/2013-01-1082
[17] Brecq G. et al., A New Indicator for Knock Detection in Gas SI Engines, *International Journal of Thermal Sciences*, 42, pp.523-532.
[18] Siano D. et al., Knock Detection Based on MAPO analysis, AR Model and Discrete Wavelet Transform Applied to the In-Cylinder Pressure Data: Results and Comparison, SAE Paper 2014-01-2547, 2014.
[19] Zhen X., et al., The engine knock analysis – An overview, *Applied Energy*, 92 (2012), pp. 628-636.
[20] Bozza et al., A Knock Model for 1D Simulations Accounting for Cyclic Dispersion Phenomena, SAE paper 2014-01-2554.
[21] Chatfield C. The Analysis of Time Series: An Introduction. 6th ed. Boca Raton, FL: Chapman & Hall/CRC, 2004
[22] Liang G. et al., ARMA model order estimation based on the eigenvalues of the covariance matrix, *IEEE Trans. Signal Process.* 41 (1993), pp. 3003–3009.
[23] Rolf S. et al., Model identification and parameter estimation of ARMA models by means of evolutionary algorithms, *Comput. Intell. Financial Eng*. 23 (1997), pp. 237–243.
[24] Akaike H., Statistical predictor identification, Ann. *Znst. Stat. Math.* 22 (1970), pp. 203–217.
[25] Spelina J. M. et al., Characterization of knock intensity distributions: Part 1: statistical independence and scalar measures, *Proceedings of the Institution of Mechanical Engineers, Part D: Journal of Automobile Engineering*, doi: 10.1177/0954407013496233, August 2013.
[26] Leppard, W., Individual-Cylinder Knock Occurence and Intensity in Multicylinder Engines, SAE Technical Paper 820074, 1982, doi:10.4271/820074.
[27] Corti E., Moro D., Knock Indexes Thresholds Setting Methodology, SAE Technical Paper 2007-01-1508, 2007, doi:10.4271/2007-01-1508.
[28] Bozza F. et al., 3D-1D Analyses of the Turbulent Flow Field, Burning Speed and Knock Occurrence in a Turbocharged SI Engine, *SAE Int. J. Engines*, section 3, vol. 116, pp. 1495-1507, 2008
[29] De Bellis V. et al., Hierarchical 1D/3D approach for the development of a turbulent combustion model applied to a VVA turbocharged engine. Part I: Turbulence model, *Energy Procedia*, Volume 45, 2014, pp. 829-838
[30] De Bellis V. et al., Hierarchical 1D/3D approach for the development of a turbulent combustion model applied to a VVA turbocharged engine. Part II: Combustion model, *Energy Procedia*, Volume 45, 2014, pp. 1027 – 1036
[31] Bozza F. et al., Numerical and Experimental Investigation of Fuel Effects on Knock Occurrence and Combustion Noise in a 2-Stroke Engine, *SAE Int. J. Fuels Lubr.*, 2012 5:674-695, doi:10.4271/2012-01-0827, ISSN: 1946-3952
[32] Fontanesi S. et al., Analysis of Knock Tendency in a Small VVA Turbocharged Engine Based on Integrated 1D-3D Simulations and Auto-Regressive Technique, *SAE Int. J. Engines* 7(1):72-86, 2014, doi:10.4271/2014-01-1065
[33] Lafossas F. et al., Development and Validation of a Knock Model in Spark Ignition Engines Using a CFD code, SAE Paper 2002-01-2701, 2002, doi: 10.4271/2002-01-2701
[34] Puzinauskas P., Examination of Methods Used to Characterize Engine Knock, SAE Paper 920808, 1992, doi:10.4271/920808.